Propensity for Helix Formation in the Hydrophobic Peptides $K_2(LA)_x$ (x = 6, 8, 10, 12) in Monolayer, Bulk, and Lipid-Containing Phases. Infrared and Circular Dichroism Studies

Darline Dieudonné, Arne Gericke,† Carol R. Flach, Xin Jiang, Ramy S. Farid,* and Richard Mendelsohn*

Contribution from the Department of Chemistry, Rutgers University, Newark College of Arts and Science, 73 Warren Street, Newark, New Jersey 07102

Received July 17, 1997. Revised Manuscript Received November 5, 1997

Abstract: A series of hydrophobic peptides $K_2(LA)_x$ (x = 6, 8, 10, 12) has been synthesized. IR and CD studies in MeOH solution are reported, along with IR studies of these species in vesicles with 1,2-dipalmitoylphosphatidylcholine, and IR Reflection−Absorption Spectroscopy (IRRAS) studies of peptide and lipid/peptide monolayer films *in situ* at the air/water interface. In bulk phases, the propensity toward helix formation increases with increasing chain length, there being essentially no helix in the shortest peptide, varying and concentration-dependent helical content in $K_2(LA)_8$, and >90% helix formation in both $K_2(LA)_{10}$ and $K_2(LA)_{12}$. In monolayers at the air/water interface, peptide secondary structure was inferred from both the Amide I and Amide A bands. The shortest peptide adopted an antiparallel β-sheet structure, while the remainder of the series (when spread at low surface pressure) appeared to adopt varying proportions of parallel β-sheet forms. The secondary structure adopted by $K_2(LA)_{10}$ and $K_2(LA)_{12}$ depended remarkably on the initial spreading pressure; when spread at high pressures, the molecules were α-helical. The current experiments demonstrate the unique advantages of IRRAS for evaluation of peptide conformations in situ at the air/water interface and reveal large differences in the propensity for helix formation in monolayers compared with bulk phases.

Introduction

Phospholipid and peptide monomolecular films at the air/water interface provide an important experimental paradigm for many fundamental processes of biological interest, such as lipid/peptide and peptide/peptide interaction.[1,2] The two-dimensional density of the molecules can be varied via lateral compression, resulting in an assortment of monolayer phases specified by various molecular orientations, conformations, domain sizes, and shapes. Determination of both molecular structure and domain size of peptides adsorbed to or imbedded in Langmuir films is an important prerequisite for addressing biological issues and for the fabrication of peptide- or protein-based biosensors.

While tendencies of peptides toward helix formation in bulk phases have been widely studied,[3] the lack of direct structural information from monolayers has limited the systematic study of secondary structure and stability of proteins and peptides at the air/water interface. To date, most conformational information about peptide and protein monolayers at the air/water interface has been obtained by determination of minimum areas from π/A-isotherms.[4−8] However, this approach is inadequate to unambiguously determine peptide or protein secondary structures. Direct information about molecular conformation/orientation can be obtained by transferring the peptide monolayer to a solid support, followed by analysis with an appropriate technique, e.g., FTIR-ATR.[9] The disadvantage of methods requiring solid supports is that the structure of monolayers at fluid interfaces depends on environmental conditions, which may alter upon film transfer. Thus, *in situ* techniques for the characterization of peptide monolayers are of importance.

The past 15 years have seen the application of a variety of in situ methods for examination of monolayer structures at the air/water interface. These include epifluorescence[10,11] and (more recently) Brewster angle microscopies[12] for evaluation of domain shape and size, and X-ray[13] and neutron scattering for the determination of tilt angles and unit cell parameters.[14] Although the above methods provide important structural details, the information generated at the level of molecular conformation and interactions is limited.

Dluhy and co-workers showed the feasibility of acquiring Infrared Reflection−Absorption Spectra (IRRAS) from monolayers at the air/water interface.[15−17] This laboratory has extended IRRAS to the study of peptide monolayer films and

† Current address: Martin-Luther-Universität Halle-Wittenberg, Institut für Physikalische Chemie, Mühlpforte 1, 06108 Halle, Germany.

(1) Jones, M. N.; Chapman, D. *Micelles, Monolayers and Biomembranes*; Wiley: New York, 1995.
(2) Möhwald, H. In *Structure and Dynamics of Membranes*; Lipowsky, R., Sackmann, E., Eds.; Elsevier: Amsterdam, 1995; pp 161−212.
(3) Haris, P. I.; Chapman, D. *Trends Biochem. Sci.* **1992**, *17*, 328−333.
(4) Ball, A.; Jones, R. A. L. *Langmuir* **1995**, *11*, 3542−3548.
(5) Gaines, G. L. *Insoluble Monolayers at liquid−gas interfaces*; Wiley: New York, 1966.
(6) Fujita, K.; Kimura, S.; Imanishi, Y.; Rump, E.; Ringsdorf, H. *Langmuir* **1994**, *10*, 2731−2735.
(7) Tronin, A.; Dubrovsky, T.; Dubrovskaya, S.; Radicchi, G.; Nicolini, C. *Langmuir* **1996**, *12*, 3272−3275.
(8) Vankann, M.; Möllerfeld, J.; Ringsdorff, H.; Höcker, H. *J. Colloid Interface Sci*. **1996**, *178*, 241−250.
(9) DeGrado, W. F.; Lear, J. D. *J. Am. Chem. Soc.* **1985**, *107*, 7684−7689.
(10) McConnell, H. M. *Annu. Rev. Phys. Chem.* **1991**, *42*, 171−195.
(11) Stine, K. J. *Microsc. Res. Technol.* **1994**, *27*, 439−450.
(12) Vollhardt, D. *Adv. Colloid Interface Sci.* **1996**, *64*, 143−171.
(13) Haas, H.; Brezesinki, G.; Möhwald, H. *Biophys. J.* **1995**, *68*, 312−314.
(14) Möhwald, H. *Annu. Rev. Phys. Chem.* **1990**, *41*, 441−476.

S0002-7863(97)02404-9 CCC: $15.00
Published on Web 01/20/1998

to mixed lipid/peptide films[18−21] and has established methods for the quantitative determination of functional group orientation.[22] IRRAS has been utilized to analyze the structural properties of some proteins;[18−21,23] however, an analysis of the influence of the peptide length on secondary structure has not appeared.

An issue that must be resolved as part of a systematic investigation of peptide structure is the inconsistency in the literature assignments for the relationship between the frequencies of the conformation-sensitive Amide I bands and peptide secondary structure. For example, for putative α-helices, the Amide I frequency occurs at ∼1635 cm^{-1} for the (hydrophilic) ribonuclease S-peptide in aqueous medium[24, 25] and at ∼1656 cm^{-1} for hydrophobic peptides in lipid bilayers.[26−28] The first assignment places the Amide I mode close to the range often quoted[29,30] for β-sheets (the latter absorb as a doublet with a strong $\nu_\perp(\pi,0)$ component near 1620−1635 cm^{-1} and a weaker $\nu_\parallel(0,\pi)$ component near 1680−1690 cm^{-1} and may be a confounding influence for the application of FT-IR to secondary structure investigations). The assignment problem is further complicated by the fact that the Amide I mode is not a pure C═O stretching vibration[31] and shifts to lower frequencies upon H → D exchange. The magnitude of the shift ranges from 3 to 12 cm^{-1}, being controlled by unknown factors. A final confounding factor is that random coil Amide I modes absorb at ∼1640−1650 cm^{-1}.

The current study reports bulk phase IR and CD studies for the series of short hydrophobic peptides $K_2(LA)_x$ (x = 6, 8, 10, and 12) in methanol solution, IR studies of these species in vesicles with 1,2-dipalmitoylphosphatidylcholine (DPPC), and IRRAS studies of peptide and lipid/peptide monolayer films in situ at the A/W interface. In addition to the fact that there is extremely limited information on the chain length dependence of peptide conformational tendencies in situ in monolayers (in either lipid or nonlipid environments), the current specific sequences were selected for several reasons. First, the peptide $K_2-(LA)_{12}-K_2-$Amide has been studied in detail[26,27] as a model for hydrophobic transmembrane helices that partition into lipid bilayers with their long axis perpendicular to the bilayer surface. Second, the sequence was expected to form easily distorted helixes which would then be more sensitive to the properties of the lipidic environment than the widely used structures $K_2-G-L_n-A-K_2-$Amide (n = 16 or 24) synthesized by Davis and co-workers.[32,33] Third, the polar residues in the current series were confined to one end of the molecule to maximize peptide insertion into lipid-containing monolayers with the helical axes parallel to the lipid acyl chains. Finally, the peptides have hydrophobic lengths of ∼18, 24, 30, and 36 Å, respectively, and thus span the hydrophobic lengths of a DPPC monolayer (∼19.7 Å in an ordered phase). Possible effects of hydrophobic mismatch on peptide conformation may therefore be studied.

Experimental Section

Materials. Purified DPPC was obtained from Avanti Polar Lipids Inc. (Alabaster, Al). The reagents and the solvents (highest purity commercially available) for peptide synthesis were obtained from Perseptive Biosystems, Inc. (Framingham, MA). Peptides were purified by using HPLC grade solvents (Aldrich, Milwaukee, WI, and Fisher Scientific, Pittsburgh, PA). Tris and sodium chloride (>99.5%) were obtained from Sigma (St. Louis, USA).

Peptide Synthesis. The peptides $K_2(LA)_x$ (x = 6, 8, 10, 12) were synthesized with use of a Millipore 9050Plus peptide synthesizer, following standard procedures for solid-phase FMOC chemistry. The amino acids were coupled as pentafluorophenyl esters in the presence of HOBt. PAL-PEG PS support resin was used to obtain neutral C-terminal carboxyamides. The peptides were deprotected and cleaved with TFA:phenol:triisopropylsilane:water (88:5:2:5) for 2 h, yielding crude protein as a major component (about 80−90% according to the integrated area of HPLC chromatograms).

Peptide Purification. The peptides were purified by reverse-phase HPLC with use of a Vydac C-18 column for the shortest peptide and a C-4 semipreparative column as required for the longer peptides in acetonitrile−water−0.1% TFA eluent gradients. The purity and identity of the peptides were confirmed by analytical HPLC and electrospray mass spectrometry. To eliminate interference in the Amide I region by the carboxy band (∼1673 cm^{-1}) of TFA, pure peptides were treated with 10 mM hydrochloric acid to replace bound TFA counterions with chloride ions.[34]

Buffer Composition. The buffer used for FT-IR experiments was 10 mM Tris, 100 mM NaCl, and 100 μM EGTA, adjusted to a pD of 7.2. D_2O (99.0% isotopic enrichment) was obtained from ISOTEC (Miamisburg, Ohio).

FT-IR Spectroscopy (Bulk Phase). Methanolic solutions of the pure peptides were prepared at concentrations ranging from 0.94 to 30 mg/mL. A fixed path length (100 μm) CaF_2 cell was used for FTIR transmission measurements. Multilamellar lipid/peptide vesicles were prepared by dissolving DPPC and the appropriate peptide in a 15:1 molar ratio in chloroform/methanol (50:50 v/v). The solvent was removed in a stream of N_2 gas and the sample was dried for several hours in high vacuum. Dry samples were rehydrated with D_2O buffer solution and vortexed to form multilamellar vesicles. CaF_2 windows with a 25 μm Teflon spacer were used to contain samples of lipid/protein mixtures for FT-IR measurements. The sample temperature was controlled by an external, manually controlled, circulating water bath (±0.1 °C). Spectra were obtained with a Mattson RS-1 (Madison, WI) spectrometer, equipped with an MCT detector. Five hundred and twelve interferograms were co-added at 4 cm^{-1} resolution and Fourier transformed with two levels of zero-filling to yield spectra encoded at ∼1 cm^{-1} intervals. For analysis of the Amide I region, buffer spectra, acquired at appropriate temperatures, were subtracted from the sample spectra. The sample and buffer matched nearly perfectly in their

(15) Mitchell, M. L.; Dluhy, R. A. *J. Am. Chem. Soc.* **1988**, *110*, 712−718.
(16) Dluhy, R. A.; Cornell, D. G. In *Fourier Transform Infrared Spectroscopy in Colloid and Interface Science*; Scheuing, D. R., Ed.; ACS Symp. Ser. 447; American Chemical Society: Washington, DC, 1991; pp 192−207.
(17) Dluhy, R. A.; Stephens, S. M.; Widayati, S.; Williams, A. D. *Spectrochim. Acta Part A* **1995**, *51*, 1413−1447.
(18) Mendelsohn, R.; Brauner, J. W.; Gericke, A. *Annu. Rev. Phys. Chem.* **1995**, *46*, 305−334.
(19) Flach, C. R.; Brauner, J. W.; Taylor, J. W.; Baldwin, R. C.; Mendelsohn, R. *Biophys. J.* **1994**, *67*, 402−410.
(20) Flach, C. R.; Prendergast, F. G.; Mendelsohn, R. *Biophys. J.* **1996**, *70*, 539−546.
(21) Gericke, A.; Flach, C. R.; Mendelsohn, R. *Biophys. J.* **1997**, *73*, 492−499.
(22) Flach, C. R.; Gericke, A.; Mendelsohn, R. *J. Phys. Chem.* **1996,** *101*, 58−65.
(23) Cornut, I.; Desbat, B.; Turlet, J. M.; Dufourcq, J. *Biophys. J.* **1996**, *70*, 305−312.
(24) Williams, S.; Causgrove, T. P.; Gilmanshin, R.; Fang, K. S.; Callender, R. H.; Woodruff, W. H.; Dyer, R. B. *Biochemistry* **1996**, *35*, 691−697.
(25) Chirgadze, Y. N.; Brazhnikov, E. V. *Biopolymers*, **1974**, *13*, 1701−1712.
(26) Zhang, Y. P.; Lewis, R. N. A. H.; Henry, G. D.; Sykes, B. D.; Hodges, R. S.; McElhaney, R. N. *Biochemistry* **1995**, *34*, 2348−2361.
(27) Zhang, Y. P.; Lewis, R. N. A. H.; Hodges, R. S.; McElhaney, R. N. *Biochemistry* **1995**, *34*, 2362−2371.
(28) Brauner, J. W.; Mendelsohn, R.; Prendergast, F. G. *Biochemistry* **1987**, *26*, 8151−8158.
(29) Fraser, R. D. B.; MacRae, T. P. *Conformation in fibrous proteins*; Academic Press: New York; 1973.
(30) Marsh, D. *Biophys. J.* **1997**, *72*, 2710−2718.
(31) Bandekar, J. *Biochim. Biophys. Acta* **1992**, *1120*, 123−143.
(32) Davis, J. H.; Clare, D. M.; Hodges, R. S.; Bloom, M. *Biochemistry* **1983**, *22*, 5298−5305
(33) Morrow, M. R.; Huschilt, J. C.; Davis, J. H. *Biochemistry* **1985**, *24*, 5396−5406

residual H_2O and HOD contents, as judged by the superposition of the respective stretching bands. The spectra were analyzed with Grams/32 software (Galactic Industries) or with additional software provided by the National Research Council of Canada.

IRRAS Measurements of Aqueous Monolayers. Peptides, either pure or mixed with DPPC in 50:50 v/v chloroform/methanol solutions, were spread onto a clean D_2O buffer subphase. The initial surface pressure after spreading the film forming material was <1 mN/m and the subphase temperature was adjusted to 21 ± 0.5 °C. IRRAS spectra were recorded with a Biorad FTS 40A (Cambridge, MA) spectrometer equipped with an MCT detector using a home-built optical attachment placed on a vibration-damped Newport I-2000 table (Fountain Valley, CA). The acquisition parameters and experimental conditions have been described in detail by Flach et al.[22] The angle of incidence was 35°, and unless noted otherwise, unpolarized radiation was used. Pure peptides $K_2(LA)_6$ (1.49 mg/mL), $K_2(LA)_8$ (1.86 mg/mL), $K_2(LA)_{10}$ (2.48 mg/mL), and $K_2(LA)_{12}$ (1.03 mg/mL) were spread at initial areas of 0.77, 2.22, 4.70 and 6.79 nm^2/molecule, respectively. After a relaxation time of 1 h, the monolayers were compressed discontinuously for ~4 h to reach a surface pressure of ~19 mN/m. Prior to data collection the monolayers were allowed to relax for at least 30 min. For experiments utilizing the single shot method,[35] samples of $K_2(LA)_6$, $K_2(LA)_8$, $K_2(LA)_{10}$, and $K_2(LA)_{12}$ were spread at areas of 0.55, 1.80, 2.12 and 1.69 nm^2/molecule, respectively, corresponding to an average $18 < \pi < 30$ mN/m.

π/A Isotherms. Peptides {$K_2(LA)_6$, 1.07 mg/mL; $K_2(LA)_8$, 0.53 mg/mL; $K_2(LA)_{10}$, 0.54 mg/mL; and $K_2(LA)_{12}$, 1.03 mg/mL} were spread from 50:50 v/v chloroform/methanol solutions onto a clean H_2O buffer solution resulting in initial areas of 1.28, 3.63, 5.53, and 11.92 nm^2/molecule, respectively. Isotherms were collected at a temperature of 21 ± 1 °C with use of a NIMA 611 trough (Coventry, UK). The compression velocity ranged from 0.026 (shortest peptide) to 0.24 nm^2 molecule^{-1} min^{-1} (longest peptide).

Circular Dichroism Spectroscopy. CD spectra were collected with an AVIV Model 60 DS spectropolarimeter with a 0.100 cm path length cell. Samples were prepared in methanol solutions and measured at ambient temperature.

Results

Solution CD and FT-IR Spectroscopy of $K_2(LA)_x$. CD spectra of $K_2(LA)_6$, $K_2(LA)_8$, and $K_2(LA)_{10}$ in methanol are shown in Figure 1.The spectrum for $K_2(LA)_6$ at higher concentrations shows the characteristic β-sheet minimum at 218 nm. Fitting the spectra in standard fashion with basis sets derived from model peptide spectra[36] reveals that the secondary structure is indeed nearly 100% β-sheet. The inset in Figure 1 shows that for $K_2(LA)_6$ the amount of β-sheet structure decreases for lower concentrations, while the amount of random coil conformation is increased. CD spectra for $K_2(LA)_{10}$ show dominant contributions from α-helical forms. For $K_2(LA)_8$ two minima are observed in the spectra. At the lowest concentrations (0.094 mg/mL), an α-helical pattern is noted with the 220 nm minimum showing a greater ellipticity than at 208 nm (not shown). However at the highest concentrations, the ellipticities at the two minima are altered from those at low concentrations. The longer wavelength band appears at 217−218 nm, slightly lower than the wavelength for a pure helical form (220 nm), suggesting that additional conformations coexist with the α-helix. Furthermore, as shown in Figure 1, the $K_2(LA)_8$ CD spectrum can be simulated from linear combinations of the spectra of $K_2(LA)_6$ (β-sheet) and $K_2(LA)_{10}$ (predominantly α-helical).

The Amide I region of the IR spectra of $K_2(LA)_6$ solutions in methanol at concentrations ranging from 0.94 to 30 mg/mL

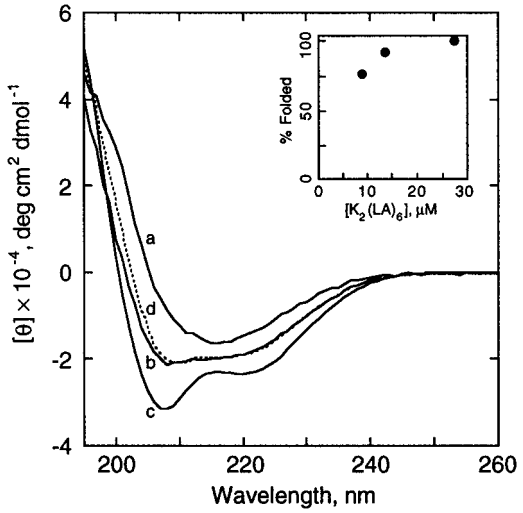

Figure 1. CD spectra of (a) $K_2(LA)_6$, (b) $K_2(LA)_8$, and (c) $K_2(LA)_{10}$ at 0.125 mg/mL in methanol. The dashed line (d) represents a fit of the $K_2(LA)_8$ spectrum, obtained as the best linear combination of $K_2(LA)_6$ (β-sheet) and $K_2(LA)_{10}$ (predominantly α-helix) spectra. The inset shows the concentration dependence of the unfolding of $K_2(LA)_6$.

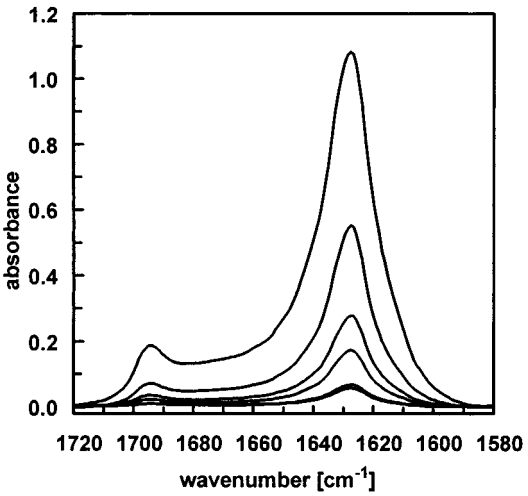

Figure 2. The spectral region 1720−1580 cm^{-1} for the dilution series of $K_2(LA)_6$ in methanol for concentrations ranging from 15 (upper curve) to 0.94 mg/mL (lowest curve).

is shown in Figure 2. The intense band at 1626 cm^{-1} is accompanied at higher concentrations by a band at 1695 cm^{-1}. At lower concentrations, the weak band diminishes in intensity to the point where detection is difficult. The presence of these two features reveals an antiparallel β-sheet structure, [31] consistent with the CD data.

IR data for $K_2(LA)_8$ solutions in methanol at concentrations ranging from 0.94 to 15 mg/mL are shown in Figure 3. The Amide I contours, in addition to containing the β-sheet doublet (1624, 1695 cm^{-1}), also exhibit a contribution from α-helical structures that appears at 1658 cm^{-1} and gains in relative intensity with successive dilution. It should be noted that the lowest concentration used in the IR experiments is somewhat higher than the concentration required for the CD measurements, i.e., the mixture of β-sheet/α-helical structures is expected. Assignment of the helical component to the 1658 cm^{-1} component of the Amide I contour is further suggested from a dilution series obtained in 2-chloroethanol solution (data not shown). This solvent, which has a greater propensity for helix formation than methanol, shows a greater proportion of 1658 cm^{-1} intensity for a given peptide concentration.

(34) Surewicz, W. K.; Mantsch, H. H.; Chapman, D. *Biochemistry* **1993**, *32*, 389−394.

(35) Gericke, A.; Simon-Kutscher, J.; Hühnerfuss, H. *Langmuir* **1993**, *9*, 3115−3121.

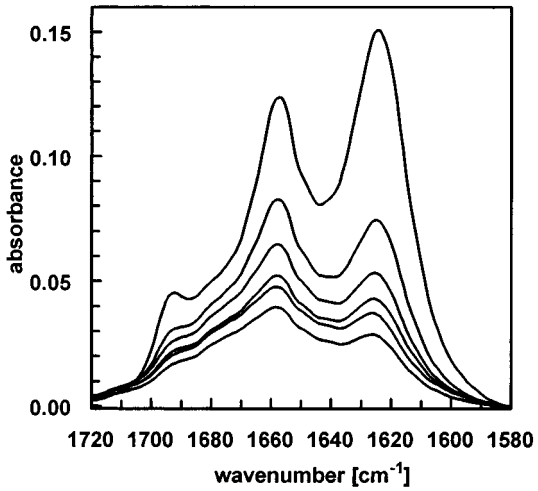

Figure 3. The spectral region 1720−1580 cm^{-1} for the dilution series of $K_2(LA)_8$ in methanol for concentrations ranging from 15 (upper curve) to 0.94 mg/mL (lowest curve).

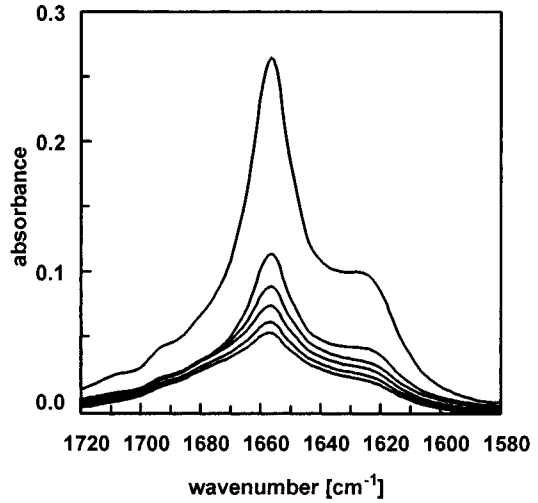

Figure 4. The spectral region 1720−1580 cm^{-1} for the dilution series of $K_2(LA)_{10}$ in methanol for concentrations ranging from 15 (upper curve) to 0.94 mg/mL (lowest curve).

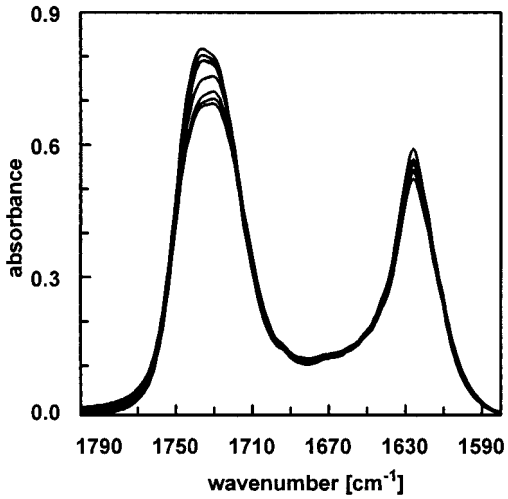

Figure 5. IR spectra for DPPC/$K_2(LA)_6$ multilamellar vesicles in D_2O buffer: spectral region of 1800−1580 cm^{-1} over the temperature range 15−55 °C (top to bottom).

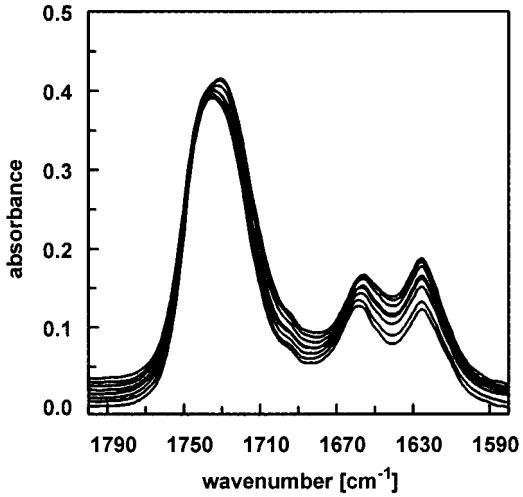

Figure 6. IR spectra for DPPC/$K_2(LA)_8$ multilamellar vesicles in D_2O buffer: spectral region of 1800−1580 cm^{-1} over the temperature range 15−55 °C (top to bottom).

The Amide I region for $K_2(LA)_{10}$ in methanol solutions for successive dilutions is shown in Figure 4. The dominant Amide I band arises from α-helical secondary structures and appears at 1659 cm^{-1}. In addition, at the higher concentrations, a band due to sheet structures appears at 1625 cm^{-1}. H → D exchange experiments in acidic CH_3OD solution showed a rather slow exchange (order of hours) for $K_2(LA)_{10}$, which was marked by a shift of the helical band position to 1649 cm^{-1} (not shown). Spectra for $K_2(LA)_{12}$ showed a dominant band at 1659 cm^{-1}. Thus, the propensity toward helix formation increases with increasing chain length, there being essentially no helix in the shortest peptide, varying, concentration-dependent amounts of helix in $K_2(LA)_8$, and >90% helix formation in both $K_2(LA)_{10}$ and $K_2(LA)_{12}$.

FT-IR Spectra of $K_2(LA)_x$ in DPPC Multilamellar Vesicles. IR spectra for $K_2(LA)_6$ in multilamellar DPPC vesicles (lipid/protein mol ratio 15:1) are shown for the 1580−1800 cm^{-1} region as a function of temperature in Figure 5. In addition to the major lipid C═O stretching band near 1730 cm^{-1}, the Amide I region depicts a doublet with a strong feature at 1628 cm^{-1} and a weaker band at 1692 cm^{-1}. The position of the $\nu_{\parallel}(0,\pi)$ band (1692 cm^{-1}) and the presence of Amide II band intensity (∼1550 cm^{-1}, not shown) indicate that the peptide is not completely H → D exchanged. IR spectra of $K_2(LA)_8$ as a function of temperature are shown in Figure 6. The Amide I region of the spectra shows two main bands, a feature at 1628 cm^{-1} ($\nu_{\perp}(\pi,0)$ of a β-sheet band) and a feature at 1658 cm^{-1} arising from α-helical structures. A fairly cooperative 20% increase in the relative intensity of the 1628 cm^{-1} band is seen in going through the lipid T_m, indicating a somewhat higher β-sheet content in fluid lipid phases. IR spectra for $K_2(LA)_{10}$ in DPPC vesicles are shown as a function of temperature in Figure 7. A single Amide I peak assigned to helical secondary structure is observed with a temperature-invariant peak position of 1657 cm^{-1}, indicating that the peptide is predominantly not H → D exchanged. Some broadening is observed on the low-frequency side, suggestive of a small fraction of β-sheet structures.

Characterization of $K_2(LA)_x$ in Pure Peptide and Peptide/DPPC Monolayers. Surface pressure/area isotherms for pure peptide monolayers are shown in Figure 8. It is found that the limiting area increases with increasing peptide length. Normalization to area/residue yields a limiting area of ≈0.04 nm^2/residue for $K_2(LA)_6$, while for $K_2(LA)_8$, $K_2(LA)_{10}$, and $K_2(LA)_{12}$ the respective values are 0.09, 0.12, and 0.16 nm^2/residue. For the short peptides these areas are considerably smaller than

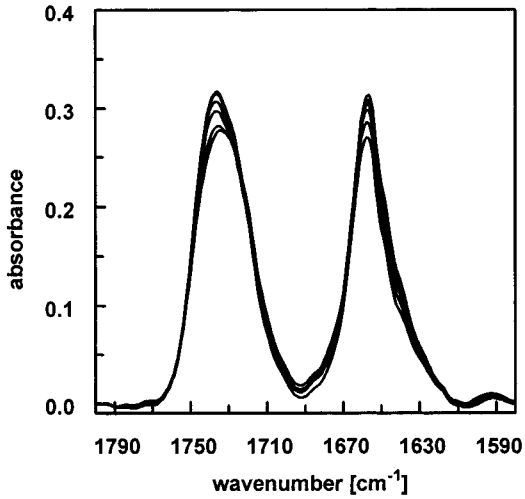

Figure 7. IR spectra for DPPC/$K_2(LA)_{10}$ multilamellar vesicles in D_2O buffer: spectral region of 1800−1580 cm^{-1} over the temperature range 15−55 °C (top to bottom).

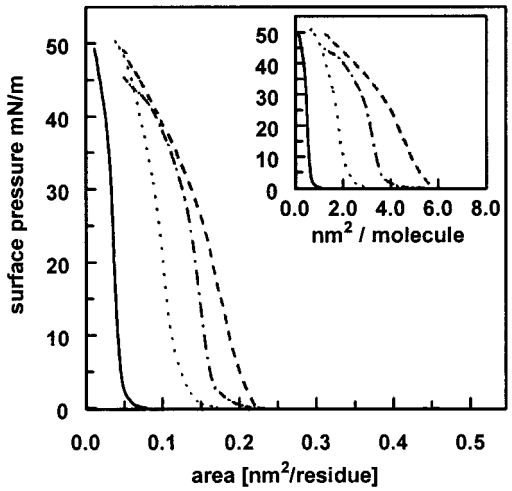

Figure 8. π/A-isotherm of $K_2(LA)_6$ (—), $K_2(LA)_8$ (···), $K_2(LA)_{10}$ (· − ·), and $K_2(LA)_{12}$ (- - -) at the air/water interface at 20.7 ± 0.1 °C. Peptides were spread from chloroform/methanol 50:50 (v/v) solutions onto an H_2O buffer subphase. Inset: π/A-isotherms normalized to area/molecule.

expected for a helical peptide monolayer with the molecules lying flat on the water, while the areas determined for the two longer peptides come close to those usually found for helical peptides[9] (especially so, considering the uncertainty in the determination of the minimum area/residue).

IRRAS spectra of $K_2(LA)_6$ in pure peptide monolayers on a D_2O subphase at various surface pressures ranging from 2.9 to 23.5 mN/m are shown in Figure 9. Peaks at 1618 and 1625 cm^{-1} are seen at all pressures, with the relative intensity of the latter increasing with increasing surface pressure. In addition, a weaker band at 1685 cm^{-1} is observed at all pressures. Spectra of this peptide in mixed monolayers with DPPC at 28 mN/m show a pattern similar to the pure peptide at 23.5 mN/m (data not shown).

Spectra of $K_2(LA)_8$ in pure peptide monolayers on a D_2O subphase at surface pressures ranging from 9.5 to 19 mN/m are shown in Figure 10. A single peak at 1618 cm^{-1}, broadened on the high-frequency side, is observed at all pressures. Similar Amide I features are observed for DPPC/$K_2(LA)_8$ mixed monolayers (not shown). Spectra obtained when pure $K_2(LA)_8$ was spread at a high initial surface pressure (single shot method)

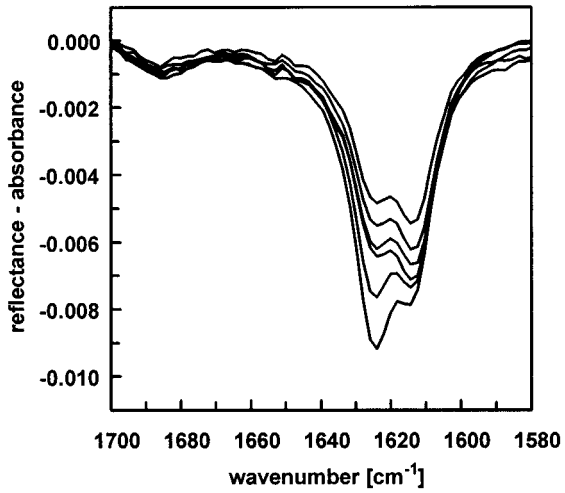

Figure 9. IRRAS spectra in the 1700−1580 cm^{-1} region for a $K_2(LA)_6$ monolayer at the air/D_2O buffer interface (21 ± 0.5 °C) at different surface pressures. The band at 1618 cm^{-1} decreases as the intensity of the peak at 1628 cm^{-1} increases with increasing pressure from 2.9 (top) to 23.5 mN/m (bottom). Unsmoothed, baseline-corrected spectra are shown.

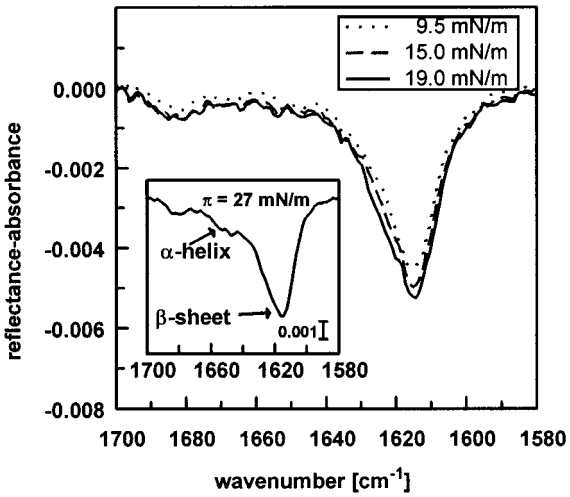

Figure 10. IRRAS spectra in the 1700−1580 cm^{-1} range for a $K_2(LA)_8$ monolayer at the air/D_2O buffer interface (21.0 ± 0.5 °C) at different surface pressures. Unsmoothed, baseline-corrected spectra are shown. The inset shows the spectrum obtained ≈1 h after spreading the peptide at π = 27 mN/m (single shot method).

revealed a dominant β-structure, with however, a small shoulder discernible at the frequency position characteristic for α-helixes (see inset Figure 10).

IRRAS spectra of $K_2(LA)_{10}$ show a remarkable sensitivity to initial spreading pressure (Figure 11). When spread at low pressures (∼0 mN/m), IRRAS spectra of both pure peptide and peptide/DPPC mixed lipid films reveal a single band at 1616 cm^{-1}, indicative of intermolecular β-sheet forms.[37] The same band position was found for $K_2(LA)_{12}$ (not shown). The intensity of the $\nu_{II}(0,\pi)$ band (≈1684 cm^{-1}) decreases for $K_2(LA)_8$ compared with $K_2(LA)_6$ and vanishes completely for $K_2(LA)_{10}$ and $K_2(LA)_{12}$.

In contrast, when $K_2(LA)_{10}$ and $K_2(LA)_{12}$ films are spread to give initial surface pressures of >15 mN/m, a slightly asymmetric Amide I band is found at 1653 cm^{-1}, consistent with

(36) Greenfield, N. J. *Anal. Biochem.* **1996,** *2355,* 1−10.
(37) Van Stokkum, I. H. M.; Linsdell, H.; Hadden, J. M.; Haris, P. I.; Chapman, D.; Bloemendahl, M. *Biochemistry* **1995**, *34,* 10508−10518.

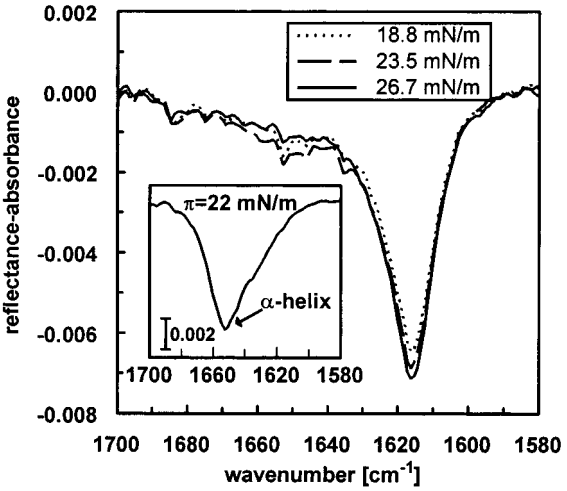

Figure 11. IRRAS spectra in the 1700−1580 cm^{-1} range for a $K_2(LA)_{10}$ monolayer at the air/D_2O buffer interface (21.0 ± 0.5 °C) at different surface pressures. Unsmoothed, baseline-corrected spectra are shown. The inset shows the spectrum obtained ≈1 h after spreading the peptide at $\pi = 22$ mN/m (single shot method).

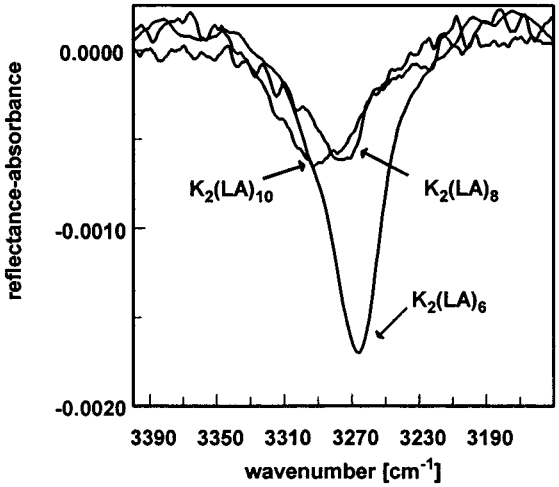

Figure 12. Amide A bands for $K_2(LA)_6$, $K_2(LA)_8$, and $K_2(LA)_{10}$ monolayers at the air/water interface (compressed state).

helical structures (see inset Figure 11). Compression of $K_2(LA)_{10}$ and $K_2(LA)_{12}$ monolayers, initially spread at low pressures, was never seen to produce an Amide I mode characteristic of an α-helical structure. When peptides were initially spread at relatively high pressures, then expanded, a fraction (10−30%) of the helical secondary structures were converted to sheet structures. Further, monolayers spread at a high surface pressure show a sharp Amide II band, indicating that these peptides are not substantially H → D exchanged. We note that spreading at high surface pressures might give rise to the formation of 3D peptide crystals.

To obtain insight into the orientation of the α-helices, s- and p-polarized spectra were acquired for $K_2(LA)_{10}$ initially spread at high surface pressures. The Amide I band for p-polarization is negatively oriented and shows no sign of a dispersion-type IRRAS band shape. This observation, along with the fact that the IRRAS intensity for p-polarized radiation is more than twice that for s-polarization, indicates that the helix tilt angle from the surface normal is >60°.[21,23]

In Figure 12, the Amide A region is shown for pure peptide films spread at low pressure. For $K_2(LA)_6$ a strong band is found at ≈3262 cm^{-1}, while for $K_2(LA)_8$ and $K_2(LA)_{10}$ considerably weaker and broader bands are observed at ≈3273 and ≈3287 cm^{-1}, respectively. Although it is impossible to determine the Amide A peak positions for $K_2(LA)_8$ and $K_2(LA)_{10}$ with high accuracy, it is obvious that, as noted, the Amide A band shifts to higher wavenumbers when the length of the peptide is increased. The Amide A band for $K_2(LA)_{10}$ spread at a high surface pressure (single shot experiment) is located at ≈3300 cm^{-1}. The Amide A mode monitors that fraction of the peptides that is not H → D exchanged.

Discussion

Three aspects of the current work will be discussed. First, spectral assignments and the propensity for helix formation in bulk phases will be considered. Second, the constraints to helix formation and the secondary structures and orientations assumed by these peptides in aqueous monolayers will be discussed. Finally, the advantages and limitations of the various experimental techniques will be evaluated.

$K_2(LA)_6$ in bulk phase is essentially completely an antiparallel β-sheet at the concentrations used for the IR measurements. At the somewhat lower concentrations used for the CD measurements the molecule begins to unfold to a random coil form, an observation which suggests that the β-sheet form is intermolecular in origin. Previous studies[38] have assigned an Amide I band near 1628 cm^{-1} in membrane proteins (e.g. porin from *Rhodobacter capsulatus*) to an intramolecular sheet form. That assignment must now be expanded to include intermolecular structures.

Helical conformations first appear for $K_2(LA)_8$ in dilute methanol solutions as indicated by a band at ∼1656 cm^{-1} that increases in relative intensity as the concentration is reduced. The interconversion between helical and sheet forms is evidently reversible as the solutions were prepared by successive dilutions. For $K_2(LA)_{10}$ and $K_2(LA)_{12}$, α-helical structures dominate at all concentrations. The current results are comparable with the work of Toniolo and co-workers, who showed that L-alanine oligomers from $n = 5$ to 8 assume a β structure, whereas the onset of α-helical structure takes place in the range $n = 10-13$.[39] Similarly, Katakai and Nakayama have observed the onset of the α-helix at the decapeptide level for 2-nitrophenylsulfenyl-$(LA)_x$OEt.[40]

The propensity for helix formation in DPPC vesicles parallels that for the MeOH solutions. The shortest peptide exists almost exclusively as a β-sheet structure. No changes in peak positions or band shapes are observed when the DPPC is warmed through its gel−liquid crystal phase transition. In contrast, $K_2(LA)_8$ exhibits both helical and β-sheet conformations. Perhaps surprisingly, the latter gains in relative intensity by about 20% as the temperature is increased through the lipid T_m. The longer peptides are overwhelmingly helical both in methanol solutions and in DPPC vesicles. The most important result of the IRRAS measurements is the observation that the propensity for helix formation in monolayer films, either in the presence or absence of phospholipids, differs substantially from the bulk phases. In monolayers of $K_2(LA)_6$, the observation of a surface pressure−sensitive doublet at 1628/1618 cm^{-1} indicates the coexistence of two extended conformations on an aqueous subphase. Bands near 1618 cm^{-1} have been associated with "aggregate" formation.[36] The molecular nature of the aggregates is unknown but the low Amide I frequency suggests the presence of strong H bonds. The increased intensity at 1628 cm^{-1} observed at higher surface pressures may result from either of two effects, namely changes in the orientation of the Amide I transition moments relative to the film normal[18] or altered surface concentrations of the two structures giving rise to the 1628 and 1618 cm^{-1}

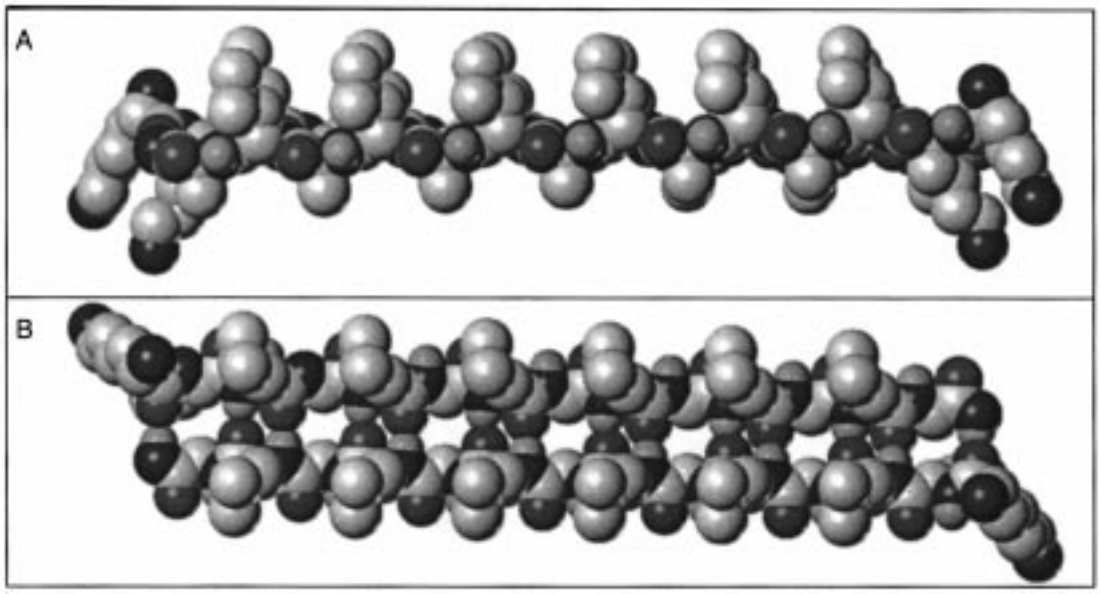

Figure 13. Space-filling representation of a model of $K_2(LA)_6$ in an antiparallel β-sheet monolayer structure at the air/water interface showing two strands. Carbon atoms are represented by light gray spheres, oxygen by medium gray, and nitrogen by dark gray. For clarity, only hydrogen atoms bound to backbone nitrogens are shown. In the side view (A) leucine side chains are shown to be directed in the air, and alanine side chains and lysine residues (at extreme left and right positions) down into the water. The top view (B) emphasizes the interchain hydrogen bonds and leucine side chain packing.

bands. It is difficult to ascertain from the current experiments which of these effects dominates. In addition, the $\nu_{||}(0,\pi)$ component at $\approx$1685 cm^{-1} reveals an antiparallel β-sheet geometry for at least one of the conformers. In addition, the presence of substantial Amide A and Amide II bands indicates that a considerable portion of the peptide is not deuterium exchanged, and is suggestive of a highly ordered structure.

The three longer peptides exhibit a single band at $\approx$1618 cm^{-1}. The integrated intensity of this band is $\sim$3 times smaller than that for the 1618/1628 cm^{-1} doublet of the $K_2(LA)_6$ monolayer. Furthermore, the $\nu_{||}(0,\pi)$ component relative intensity is reduced for $K_2(LA)_8$ compared to the shortest peptide and vanishes for $K_2(LA)_{10}$ and $K_2(LA)_{12}$. IRRAS intensities are governed by the number of molecules in the beam area and the direction of the transition dipole moment relative to the surface. The progressive reduction in intensity with increasing number of residues is unlikely to result from the occurrence of a particular orientation that effectively eliminates the IRRAS intensity. A plausible alternative explanation is that a parallel β-sheet structure forms for the longer peptides. The $\nu_{||}(0,\pi)$ band for a parallel β-sheet is calculated at $\approx$1645 cm^{-1} and may be visible as a weak shoulder on the main β-sheet band.[41] Such a shoulder would be difficult to discern from IRRAS measurements.

Additional secondary structure information is gained from the Amide A band positions, although spectra−structure correlations are less well established than for the Amide I band. A further caveat is that Amide A frequencies on a D_2O subphase reflect only the conformations of unexchanged peptide bonds. Bulk phase measurements for short peptides forming antiparallel and parallel intermolecular β-sheets indicate that the Amide A frequency for the former occurs between 3260 and 3280 cm^{-1}, while for the latter, the frequency ranges from 3280 to 3295 cm^{-1}.[9,42] The corresponding frequency range for α-helixes is further increased by 10−20 cm.[1]

A sharp Amide A band appears at 3262 cm^{-1} for $K_2(LA)_6$. Along with the Amide I frequency data, the IRRAS results from the two spectral regions are consistent and suggest an antiparallel sheet structure. A model for the $K_2(LA)_6$ antiparallel β-sheet monolayer consistent with the data is depicted in Figure 13. The isobutyl side chains of the leucines point toward the air, while the alanine methyl groups are directed into the water. The lysine groups of the peptides are well separated and are also directed into the aqueous phase. The observed area/residue is small for this assembly (because the bulky isobutyl groups point into the air) in good agreement with π/A-measurements. The transition moment direction for the Amide I is in the plane of the water interface (x,y plane), resulting in maximum IRRAS band intensities for the experimental conditions (angle of incidence 35°, unpolarized radiation[18]). Coupled with the fact that $K_2(LA)_6$ possesses an antiparallel β-structure in the spreading solution, the structure in Figure 13 appears quite reasonable. For $K_2(LA)_8$, a very broad Amide A band is observed at $\approx$3275 cm^{-1} while the same band for $K_2(LA)_{10}$ (spread at low surface pressure) is located at 3287 cm^{-1}. Considering the absence of a $\nu_{||}(0,\pi)$ Amide I band at $\approx$1685 cm^{-1}, it is likely that $K_2(LA)_{10}$ exhibits a parallel β-sheet structure when compressed from low surface pressures. For $K_2(LA)_8$, because of the intermediate Amide A frequency and the weak, $\nu_{||}(0,\pi)$ band, the situation is less clear, although the best conjecture is that both parallel and antiparallel β-structures are present at the air/water interface. The α-helical $K_2(LA)_{10}$ monolayer (spread at high surface pressures) has a broad Amide A band observed at $\sim$3300 cm^{-1}, consistent with the suggested assignment.

A tentative structural model for the longer peptides is given below. The π/A-isotherms of $K_2(LA)_8$, $K_2(LA)_{10}$, and $K_2(LA)_{12}$ are more characteristic of an expanded film structure than the $K_2(LA)_6$ monolayer, which is quite condensed. While structural

(38) Haris, P. I.; Chapman, D. In *Infrared Spectroscopy of Biomolecules;* Mantsch, H. H., Chapman, D., Eds.; Wiley-Liss: New York, 1996; pp 239−278.

(39) Bonora, G. M.; Palumbo, M.; Toniolo, C.; Mutter, M. *Makromol. Chem.* **1979**, *180*, 1293−1296.

(40) Katakai, R.; Nakayama, Y. J. *J. Chem. Soc., Chem. Commun.* **1977**, 805−807.

(41) Qian, W.; Bandekar, J.; Krimm, S. *Biopolymers* **1991**, *31*, 193−210.

(42) Toniolo, C.; Palumbo, M. *Biopolymers* **1977**, *16*, 219−224.

conclusions based solely on π/A-isotherms are subject to uncertainty because of factors such as peptide dissolution into the subphase, and deviations from ideal packing geometry, the area/residue is nevertheless considerably larger for the longer peptides, which suggests a structure different from an assembly such as that depicted in Figure 13 for $K_2(LA)_6$. Isotherms for the longer peptides produce an area/residue that could be deduced as arising from helical structures with the molecules lying flat on the water, a conclusion completely incompatible with the IRRAS data.

Parallel β-structures, in which the lysine residues are aligned at one end of the sheet, can adopt any orientation with respect to the water surface. In the current instance, both the IRRAS intensities (compared to $K_2(LA)_6$) and the π/A-isotherms indicate that the β-sheet is rotated out of the plane of the water. For such geometries the isobutyl side chains of the leucines prevent the peptides from close packing. The film will therefore be expanded and the IRRAS intensities will be diminished due to both lower surface density and transition moment direction effects.[22]

A possible reason for the different geometry adopted by $K_2(LA)_6$ compared with the other peptides is the different secondary structure adopted in the spreading solvent (antiparallel β-structure vs helical). $K_2(LA)_6$ maintains its solution structure in monolayers as shown by the persistence of the 1628 cm^{-1} band and by the fact that the peptide is largely unexchanged in D_2O. In contrast, the longer peptides would have to unfold and reassemble to form an antiparallel β-sheet. The preference of the longer peptides for a parallel β-structure might be due to submersion of the lysines of the initially helical peptides into the water. In single shot experiments, where the spreading process is impeded by the reduced area/molecule, the longer peptides retain the conformation adopted in the spreading solvents. Notably, spreading of $K_2(LA)_8$ at high surface pressure (single shot experiment) yielded a mixture of helical and β-structures, consistent with the idea that the structure found in solution is maintained in the early stages of the spreading process at the air/water interface.

The peptides described in this paper show a remarkable tendency to unfold and aggregate at the air/water interface, in contrast to studies of other peptides of comparable length. For example, Cornut et al. investigated an amphipathic KLLKLLLKLL$(KLLL)_2$KLLK monolayer by IRRAS and found a helical structure with an orientation parallel to the water surface.[23] Since lysine residues are known to support helical structures, the 7 residues present presumably stabilize this structure at the air/water interface.[43] In addition, Fujita et al. investigated transferred films of amphipathic peptides with different lengths and with the repeating sequences Ala-Aib and Lys(Z)-Aib.[44] This preparation yielded helixes which lay flat on the aqueous surface. Finally, DeGrado and Lear investigated some amphipathic helical peptides and found this secondary structure to be maintained in transferred films.[9]

The observation of helical structures at the A/W interface is not, however, confined to amphipathic molecules. In an IRRAS study from this laboratory, the secondary structure of the lung surfactant protein C (SP−C) (containing a hydrophobic, 27-residue, valine-rich, helical sequence along with a hydrophilic, charged, 8-residue extended region) was shown to be unchanged in going from bulk phases to monolayer films at the air/water interface.[21] The helix axis was tilted 72° from the surface normal. The lack of aggregation in this peptide is presumably related to electrostatic repulsion between the charged residues.

In summary, IRRAS offers a unique opportunity for evaluation of peptide conformations in situ at the A/W interface, without the necessity for transferring films to a solid substrate. Peptide conformations are deduced from spectra-structure correlations of the Amide I modes. These correlations are quite reliable for β-structures, but less so for α-helixes, as noted in the Introduction. Thus, the use of complementary experimental approaches is helpful. In the current study, comparison of CD with IR spectra in methanol solutions engenders some confidence in the IR spectra−structure correlations for helixes, and in the transferability of the spectra−structure correlations to IRRAS experiments. If CD spectra cannot be acquired due to spectral distortions (membrane vesicles) or inadequate sensitivity (monolayers), a comparison of Amide I with Amide A frequencies may prove helpful. More generally, a molecular level understanding of the factors controlling peptide aggregation in monolayers would seem to be of interest with regard to their utilization as biosensors.

Acknowledgment. This work was supported by grant GM 29864 to R.M. from the Public Health Service. A.G. was supported by a grant from the Deutsche Forschungsgemeinschaft.

JA9724046

(43) Creighton, T. E. *Proteins*; W. H. Freeman: New York, 1984.
(44) Fujita, K.; Kimura, S.; Imanishi, Y.; Okamura, E.; Umemura, J. *Langmuir* **1995**, *11*, 1675−1679.